

Observation of In-Plane Quantum Griffiths Singularity in Two-Dimensional Crystalline Superconductors

Yi Liu,^{1,2} Shichao Qi,¹ Jingchao Fang,¹ Jian Sun[ⓧ],¹ Chong Liu[ⓧ],³ Yanzhao Liu,¹ Junjie Qi,⁴ Ying Xing,⁵ Haiwen Liu,^{6,†} Xi Lin,^{1,4,7} Lili Wang[ⓧ],³ Qi-Kun Xue,^{3,4} X. C. Xie,^{1,4,7} and Jian Wang[ⓧ]^{1,4,7,*}

¹International Center for Quantum Materials, School of Physics, Peking University, Beijing 100871, China

²Department of Physics, Renmin University of China, Beijing 100872, China

³State Key Laboratory of Low-Dimensional Quantum Physics, Department of Physics, Tsinghua University, Beijing 100084, China

⁴Beijing Academy of Quantum Information Sciences, Beijing 100193, China

⁵Department of Materials Science and Engineering, College of New Energy and Materials, China University of Petroleum, Beijing 102249, China

⁶Center for Advanced Quantum Studies, Department of Physics, Beijing Normal University, Beijing 100875, China

⁷CAS Center for Excellence in Topological Quantum Computation, University of Chinese Academy of Sciences, Beijing 100190, China

 (Received 2 November 2020; revised 27 January 2021; accepted 9 August 2021; published 24 September 2021)

Quantum Griffiths singularity (QGS) reveals the profound influence of quenched disorder on the quantum phase transitions, characterized by the divergence of the dynamical critical exponent at the boundary of the vortex glasslike phase, named as quantum Griffiths phase. However, in the absence of vortices, whether the QGS can exist under a parallel magnetic field remains a puzzle. Here, we study the magnetic field induced superconductor–metal transition in ultrathin crystalline PdTe₂ films grown by molecular beam epitaxy. Remarkably, the QGS emerges under both perpendicular and parallel magnetic field in four-monolayer PdTe₂ films. The direct activated scaling analysis with a new irrelevant correction has been proposed, providing important evidence of QGS. With increasing film thickness to six monolayers, the QGS disappears under perpendicular field but persists under parallel field, and this discordance may originate from the differences in microscopic processes. Our work demonstrates the universality of parallel field induced QGS and can stimulate further investigations on novel quantum phase transitions under parallel magnetic field.

DOI: [10.1103/PhysRevLett.127.137001](https://doi.org/10.1103/PhysRevLett.127.137001)

Two-dimensional (2D) crystalline superconductors [1] are ideal platforms to study the quantum phase transition, a continuous phase transition at absolute zero temperature [2,3]. As a prototype of quantum phase transition, the superconductor–insulator or superconductor–metal transition (SIT or SMT) has been widely and intensely investigated, where the quantum fluctuations play a dominant role and determine its characteristics [4,5]. The recent observations of quantum Griffiths singularity (QGS) of SMT in low-dimensional superconducting systems [6–13], characterized by a divergent critical exponent $z\nu$, challenge the conventional understanding of the quantum phase transition. QGS reveals the profound influence of the quenched disorder on SMT, which originates from the disorder driven evolution from vortex lattice to vortex glasslike phase, named as quantum Griffiths phase. The quantum Griffiths phase consists of large superconducting rare regions and the surrounding normal state. The size of these superconducting regions keeps increasing with decreasing temperature to zero, and the slow dynamics leads to a divergent critical exponent $z\nu$ of SMT in 2D systems [14,15], in contrast to the

constant $z\nu$ observed in conventional quantum phase transitions [2,3]. The previous experimental works focus on the observation of QGS under perpendicular magnetic field. Under parallel field, the experimental investigation of QGS in the absence of vortices in 2D crystalline superconductors is highly desired.

In this Letter, we report the transport properties of 4- and 6-monolayer (ML) PdTe₂ films via ultralow temperature transport measurement. Remarkably, the divergence of critical exponent $z\nu$ as an evidence of QGS is detected in 4-ML PdTe₂ films under both perpendicular and parallel magnetic field. Moreover, the QGS is directly identified by the activated scaling analysis with a new irrelevant correction. Interestingly, with increasing film thickness, the QGS disappears in the 6-ML film under perpendicular field but still exists under parallel field, revealing different microscopic processes of QGS under different field directions. We propose that the disorder can significantly influence the strength of spin-orbit coupling (SOC) and the in-plane critical field, which gives rise to the quantum Griffiths phase without vortex formation.

The ultrathin crystalline PdTe₂ films were epitaxially grown on Nb-doped SrTiO₃(001) substrates in the ultra-high vacuum molecular beam epitaxy chamber (see Supplemental Material, Methods for details [16]). The morphology of the PdTe₂ films is characterized by the scanning tunneling microscope [20]. The PdTe₂ thin films are ambient-stable superconductors, which do not require a capping layer for *ex situ* transport measurement. Figure 1 presents the superconducting properties of 4-ML PdTe₂ film, measured in a dilution refrigerator (MNK 126-450; Leiden Cryogenics BV) down to 20 mK. The standard four-electrode transport measurements are schematically shown in the inset of Fig. 1(c) (see Supplemental Material, Methods for details [16]). The superconducting transition begins at $T_c^{\text{onset}} = 700$ mK, which is defined as the crossing point of the linear extrapolations of normal state and superconducting transition curve. With decreasing temperature, the sheet resistance drops to zero within the measurement resolution at $T_c^{\text{zero}} = 570$ mK. As the perpendicular magnetic field increases, the 4-ML PdTe₂ film undergoes a superconductor to weakly localized metal transition with a quantum critical resistance (around 977 Ω) much smaller than the quantum resistance for Cooper pairs ($h/4e^2 \sim 6.45$ kΩ, where h is the Planck

constant and e is the elementary charge), as shown in the inset of Fig. 1(a). The sheet resistance increases with decreasing temperature when the magnetic field exceeds 0.98 T, indicating localized metal behavior. The perpendicular magnetic field dependence of sheet resistance at different temperatures from 20 to 450 mK is displayed in Fig. 1(b) (see Supplemental Material, Fig. S1 for the magnetoresistance in a large magnetic field region [16]). Different from conventional SMT, the magnetoresistance isotherms cross each other in a relatively large and well-defined transition region around 0.9 T at low temperatures rather than a single critical point, reminiscent of QGS. The crossing points of $R_s(B)$ curves at neighboring temperatures are shown as black dots in the inset of Fig. 1(b). Furthermore, based on the finite size scaling analysis [2,3,16], the magnetic field dependence of the effective “critical” exponent $z\nu$ is summarized in Fig. 1(c). When approaching the characteristic magnetic field B_c^* and zero temperature, $z\nu$ grows rapidly and then diverges. The field dependence of $z\nu$ can be well fitted by the activated scaling law $z\nu \propto |B_c^* - B|^{-\nu\psi}$ with the correlation length exponent $\nu \approx 1.2$ and the tunneling critical exponent $\psi \approx 0.5$ for 2D systems [21,22], providing experimental evidence of QGS in the 4-ML PdTe₂ film under perpendicular

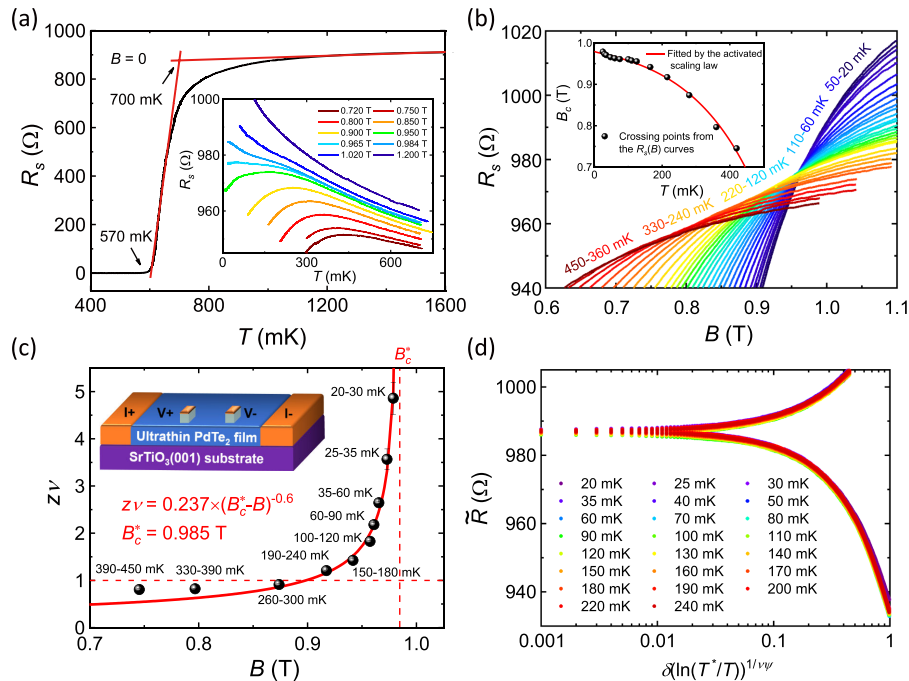


FIG. 1. The QGS of 4-ML PdTe₂ film under perpendicular magnetic field. (a) Temperature dependence of sheet resistance R_s at zero magnetic field, showing $T_c^{\text{onset}} = 700$ mK and $T_c^{\text{zero}} = 570$ mK. Inset: $R_s(T)$ curves at various magnetic fields from 0.720 to 1.200 T. (b) $R_s(B)$ curves at detailed temperatures ranging from 20 to 450 mK. Crossing points from the $R_s(B)$ curves are shown in the inset. The solid red line is the fitting curve from the activated scaling analysis with irrelevant correction. (c) Critical exponent $z\nu$ as a function of perpendicular field. The solid red line shows a fitting curve based on the activated scaling law and gives $B_c^* = 0.985$ T (vertical dashed line). The horizontal dashed red line shows $z\nu = 1$. Inset: The schematic for standard four-electrode transport measurements. (d) The direct activated scaling analysis of the $R_s(B)$ curves from 20 to 240 mK with the irrelevant correction. Here, \tilde{R} represents the sheet resistance considering the irrelevant correction and $\delta = |B - B_c^*|$.

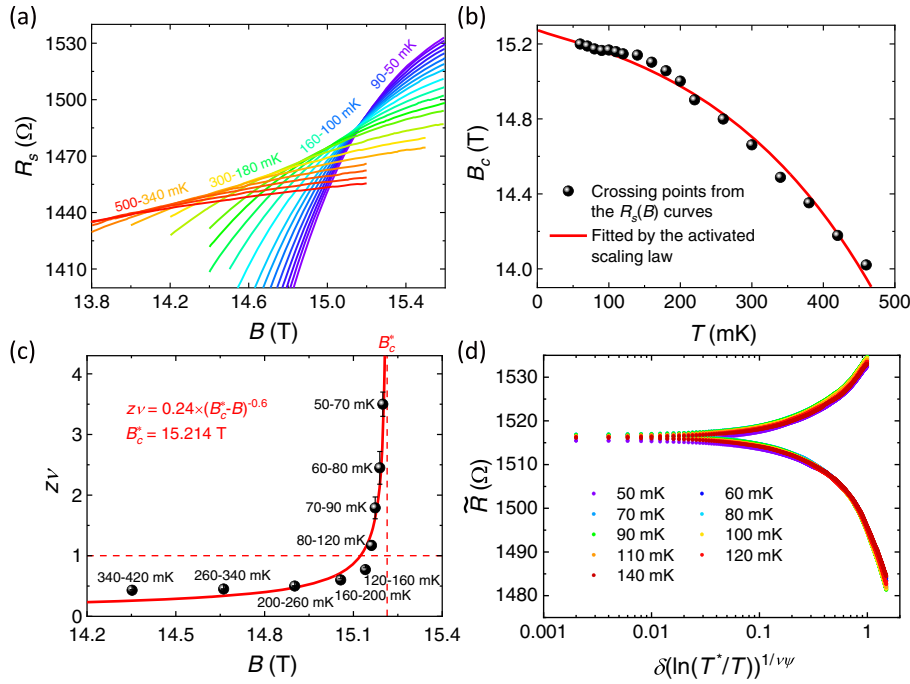


FIG. 2. The QGS of 4-ML PdTe₂ film under parallel magnetic field. (a) Parallel magnetic field dependence of R_s at different temperatures. (b) Crossing points from the magnetoresistance isotherms. The solid red line is the fitting curve from the activated scaling analysis with irrelevant correction. (c) Critical exponent $z\nu$ obtained from finite size scaling analysis. The solid red line shows a fitting curve based on the activated scaling law and gives $B_c^* = 15.214$ T (vertical dashed line). The horizontal dashed red line shows $z\nu = 1$. (d) The direct activated scaling analysis of the $R_s(B)$ curves from 50 to 140 mK with the irrelevant correction. Here, \tilde{R} represents the sheet resistance considering the irrelevant correction and $\delta = |B - B_c^*|$.

magnetic field with the infinite-randomness quantum critical point. We define the QGS under perpendicular (out-of-plane) field as the out-of-plane QGS. The out-of-plane QGS is confirmed in another 4-ML PdTe₂ film as shown in Supplemental Material, Fig. S2 [16].

The divergence of effective critical exponents $z\nu$ near the quantum critical point originates from the activated scaling behavior of QGS [23]. Thus, we utilize the direct activated scaling analysis with the irrelevant parameter correction as follows [13]: $R = \Phi\{[(B - B_c^*)/B_c^*][\ln(T^*/T)]^{(1/\nu\psi)}, u[\ln(T^*/T)]^{-y}\}$. Here, T^* is the characteristic temperature of quantum fluctuation, u is the leading irrelevant scaling variable and $y > 0$ is the associate irrelevant exponent. (See Supplemental Material Part II for detailed numerical scaling procedure [16].) The irrelevant correction also gives a good fitting for the phase boundary $B_c(T)$ of superconductor-metal transition [13]: $\{[B_c^* - B_c(T)]/B_c^*\} \propto u[\ln(T^*/T)]^{-(1/\nu\psi)-y}$. The fitting of $B_c(T)$ is shown in the inset of Fig. 1(b). The activated scaling of twenty-three sets of data in the temperature range from 20 to 240 mK is presented in Fig. 1(d), providing direct evidence of QGS.

We then investigate the superconducting properties of 4-ML PdTe₂ films under parallel magnetic fields up to 16 T in a commercial physical property measurement system with dilution refrigerator option down to 50 mK. Interestingly, as shown in Fig. 2, the film exhibits the characteristics of

QGS, which is quite similar to the observations under perpendicular field. To be specific, the $R_s(B)$ curves at different temperatures reveal a large transition region in Fig. 2(a) and the crossing points are consistent with the activated scaling model with irrelevant corrections as shown in Fig. 2(b). Moreover, the effective critical exponent $z\nu$ follows the activated scaling law $z\nu \propto |B_c^* - B|^{-0.6}$ when approaching characteristic field B_c^* and zero temperature [Fig. 2(c)]. The direct activated scaling analysis with irrelevant corrections [Fig. 2(d)] and the divergence of $z\nu$ provide solid evidence of QGS under parallel magnetic field (named as in-plane QGS).

The detection of the out-of-plane and in-plane QGS in 4-ML PdTe₂ films indicates the universality of QGS under different field orientations. It is noteworthy that the vortex-lattice phase can evolve into vortex-glass phase driven by quenched disorder under perpendicular magnetic field, which finally leads to QGS. However, this theoretical scenario does not work under parallel field where the vortex is absent, suggesting a different microscopic mechanism for in-plane QGS. Further exploration of QGS with different sample thickness may provide essential information for understanding the origin of in-plane QGS.

Thus, we performed ultralow temperature transport measurements on 6-ML PdTe₂ films. Figures 3(a) and 3(b) show the SMT behavior of the 6-ML PdTe₂ film under

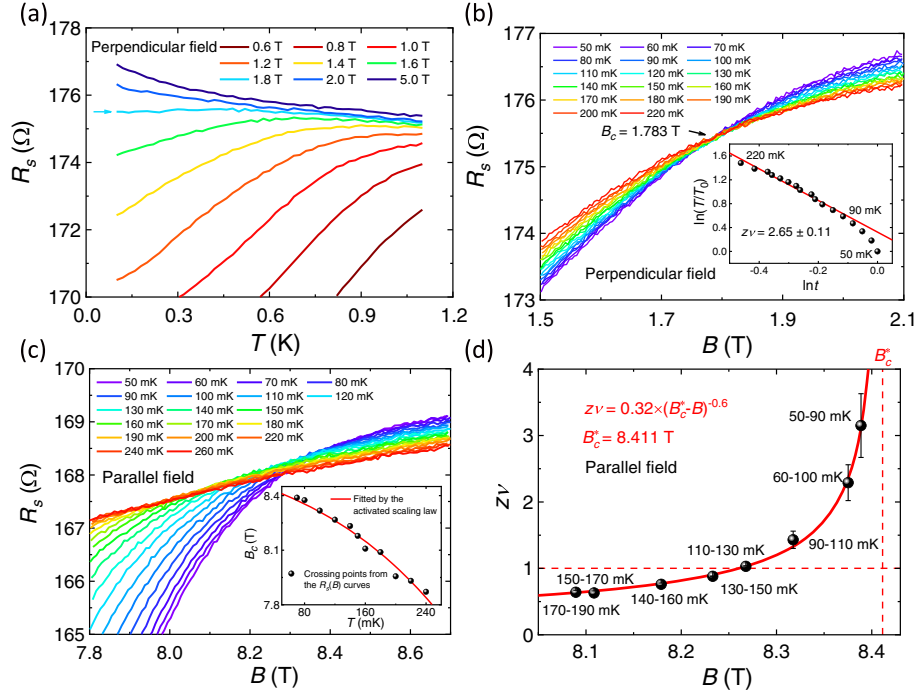


FIG. 3. Transport properties of 6-ML PdTe₂ film under perpendicular and parallel magnetic field. (a) $R_s(T)$ curves under perpendicular field ranging from 0.6 to 5.0 T. The arrow indicates a plateau where R_s remains nearly a constant at low temperatures. (b) $R_s(B)$ curves under perpendicular field at various temperatures, exhibiting one crossing point at $B_c = 1.783$ T. Inset: the temperature dependence of the scaling parameter $t[t = (T/T_0)^{-1/z\nu}]$. The solid red line is the linear fitting from 90 to 220 mK, showing $z\nu$ around 2.65. (c) The parallel magnetic field dependence of R_s at different temperatures. Crossing points from $R_s(B)$ curves are shown in the inset. The solid red line is the fitting curve from the activated scaling analysis with irrelevant correction. (d) Critical exponent $z\nu$ obtained from scaling analysis. The solid red line shows a theoretical fitting based on the activated scaling law and gives $B_c^* = 8.411$ T (vertical dashed line). The horizontal dashed red line shows $z\nu = 1$.

perpendicular field. During the SMT, the $R_s(T)$ curve at 1.8 T exhibits a plateau in a relatively large temperature regime at ultralow temperatures, corresponding to a single crossing point of the $R_s(B)$ curves below 220 mK. Finite size scaling in the inset of Fig. 3(b) further demonstrates a single value of $z\nu$ around 2.65 (the absolute value of the slope of the solid red line) between 90–220 mK (see details in Fig. S6 [16]), consistent with the quantum percolation theory [24–26]. However, $z\nu$ increases at lower temperatures below 90 mK. The above observation indicates that the characteristics of the out-of-plane QGS disappear with increasing film thickness, which very likely results from the relatively weak quantum fluctuation and disorder in thicker films. The Ioffe-Regel parameters are presented in Table S2 [16], revealing relatively weak disorder in the 6-ML PdTe₂ film. Interestingly, the main characteristic of in-plane QGS (i.e., the activated scaling law of $z\nu$) still persists in the same 6-ML PdTe₂ film under parallel magnetic field [Figs. 3(c) and 3(d)]. The emergence of QGS is also confirmed by the direct activated scaling analysis with the irrelevant correction, as shown in the inset of Fig. 3(c) and Fig. S7.

This discordance may originate from the different microscopic processes driven by disorder under different magnetic field orientations. Under perpendicular magnetic

field, the disorder effect can deform the vortex lattice and give rise to a vortex glasslike phase, where the large superconducting rare regions lead to the divergence of critical exponent $z\nu$. Compared to the QGS under perpendicular field, the different thickness dependent behavior as well as the absence of vortices in ultrathin 2D systems indicates a new mechanism of in-plane QGS. The mechanism of QGS without vortex has been theoretically revealed in superconducting nanowires, which can be extended to 2D superconductors [27]. Moreover, the ultrathin crystalline PdTe₂ films are type-II Ising superconductors with strong SOC [20,28]. The threefold rotational symmetry of PdTe₂ films makes the effective field of Zeeman-type SOC along the out-of-plane direction, which protects the superconductivity under the large in-plane magnetic field. The in-plane critical field of PdTe₂ films depends on the effective Zeeman-type SOC $\widetilde{\beta}_{\text{SO}} = \beta_{\text{SO}}/[1 + \hbar/(2\pi k_B T_c \tau_0)]$ [20,29]. Here, β_{SO} is the strength of Zeeman-type SOC, τ_0 is the mean free time for spin-independent scattering, and T_c is the superconducting critical temperature. Because of the different local disorder strength with different value of τ_0 , the local effective SOC $\widetilde{\beta}_{\text{SO}}$ varies with location. When the in-plane magnetic field is near the mean-field critical field, the regions with

relatively large disorder are easier to lose superconductivity and form the normal state, while the others keep superconducting and form the rare regions. The formation of rare regions under parallel field may give rise to the in-plane QGS. The disorder on the film surface and the interface between the film and the substrate may play a more important role in thinner films. Besides, the strain due to lattice mismatch between the film and substrate may lead to lattice distortion and finally contribute to the strength of disorder [30]. With decreasing film thickness, the strain is enhanced and thus the disorder strength is increased.

In conclusion, we systematically investigate the SMT behavior of ultrathin crystalline PdTe₂ films. Intriguingly, the QGS is observed in 4-ML PdTe₂ film under both perpendicular and parallel magnetic fields. The evidence of QGS is also provided by a direct activated scaling analysis. With increasing film thickness, the out-of-plane QGS disappears while the in-plane QGS still exists in the 6-ML PdTe₂ film, indicating a new microscopic mechanism for the in-plane QGS. Our findings shed new light on the formation of QGS and inspire further investigations on the quantum phase transition under parallel magnetic field.

We thank Yaochen Li, Pengjie Wang, Cheng Chen, and Zihan Cui for the help in transport measurement and data analysis. This work was financially supported by the National Key Research and Development Program of China (Grants No. 2018YFA0305604, No. 2017YFA0303300, No. 2017YFA0304600), the National Natural Science Foundation of China (Grants No. 11888101, No. 11774008, No. 12174442, No. 11974430, No. 12022407), Beijing Natural Science Foundation (Z180010), the Strategic Priority Research Program of Chinese Academy of Sciences (Grant No. XDB2800000) and China Postdoctoral Science Foundation (Grants No. 2019M650290 and No. 2020T130021).

Yi L. and S. Q. contributed equally to this work.

Note added in the proof.—After we submitted this Letter, we noted the observation of in-plane QGS signature in a polycrystalline superconducting film [31].

*Corresponding author.

jianwangphysics@pku.edu.cn

†Corresponding author.

haiwen.liu@bnu.edu.cn

- [1] Y. Saito, T. Nojima, and Y. Iwasa, *Nat. Rev. Mater.* **2**, 16094 (2016).
- [2] S. L. Sondhi, S. M. Girvin, J. P. Carini, and D. Shahar, *Rev. Mod. Phys.* **69**, 315 (1997).
- [3] S. Sachdev, *Quantum Phase Transitions* (Cambridge University Press, Cambridge, England, 1999).
- [4] A. M. Goldman, *Int. J. Mod. Phys. B* **24**, 4081 (2010).
- [5] A. Del Maestro, B. Rosenow, and S. Sachdev, *Ann. Phys. (Berlin)* **324**, 523 (2009).

- [6] Y. Xing, H.-M. Zhang, H.-L. Fu, H. Liu, Y. Sun, J.-P. Peng, F. Wang, X. Lin, X.-C. Ma, Q.-K. Xue, J. Wang, and X. C. Xie, *Science* **350**, 542 (2015).
- [7] N. Markovic, *Science* **350**, 509 (2015).
- [8] S. Shen, Y. Xing, P. Wang, H. Liu, H. Fu, Y. Zhang, L. He, X. C. Xie, X. Lin, J. Nie, and J. Wang, *Phys. Rev. B* **94**, 144517 (2016).
- [9] Y. Xing, K. Zhao, P. Shan, F. Zheng, Y. Zhang, H. Fu, Y. Liu, M. Tian, C. Xi, H. Liu, J. Feng, X. Lin, S. Ji, X. Chen, Q.-K. Xue, and J. Wang, *Nano Lett.* **17**, 6802 (2017).
- [10] Y. Saito, T. Nojima, and Y. Iwasa, *Nat. Commun.* **9**, 778 (2018).
- [11] E. Zhang, J. Zhi, Y.-C. Zou, Z. Ye, L. Ai, J. Shi, C. Huang, S. Liu, Z. Lin, X. Zheng, N. Kang, H. Xu, W. Wang, L. He, J. Zou, J. Liu, Z. Mao, and F. Xiu, *Nat. Commun.* **9**, 4656 (2018).
- [12] Y. Liu, Z. Wang, P. Shan, C. Liu, Y. Tang, C. Chen, Y. Xing, Q. Wang, H. Liu, X. Lin, X. C. Xie, and J. Wang, *Nat. Commun.* **10**, 3633 (2019).
- [13] N. A. Lewellyn, I. M. Percher, J. J. Nelson, J. Garcia-Barriocanal, I. Volotsenko, A. Frydman, T. Vojta, and A. M. Goldman, *Phys. Rev. B* **99**, 054515 (2019).
- [14] D. S. Fisher, *Phys. Rev. B* **51**, 6411 (1995).
- [15] T. Vojta, C. Kotabage, and J. A. Hoyos, *Phys. Rev. B* **79**, 024401 (2009).
- [16] See Supplemental Material at <http://link.aps.org/supplemental/10.1103/PhysRevLett.127.137001> for details, which includes Refs. [17–19].
- [17] K. Slevin and T. Ohtsuki, *Phys. Rev. Lett.* **82**, 382 (1999).
- [18] Y. Saito, Y. Kasahara, J. T. Ye, Y. Iwasa, and T. Nojima, *Science* **350**, 409 (2015).
- [19] R. A. Klemm, *Layered Superconductors* (Oxford University Press, Oxford, 2012).
- [20] Y. Liu, Y. Xu, J. Sun, C. Liu, Y. Liu, C. Wang, Z. Zhang, K. Gu, Y. Tang, C. Ding, H. Liu, H. Yao, X. Lin, L. Wang, Q.-K. Xue, and J. Wang, *Nano Lett.* **20**, 5728 (2020).
- [21] T. Vojta, A. Farquhar, and J. Mast, *Phys. Rev. E* **79**, 011111 (2009).
- [22] I. A. Kovacs and F. Igloi, *Phys. Rev. B* **82**, 054437 (2010).
- [23] D. S. Fisher, *Physica (Amsterdam)* **263A**, 222 (1999).
- [24] K. Slevin and T. Ohtsuki, *Phys. Rev. B* **80**, 041304(R) (2009).
- [25] M. Amado, A. V. Malyshev, A. Sedrakyan, and F. Dominguez-Adame, *Phys. Rev. Lett.* **107**, 066402 (2011).
- [26] H. Obuse, I. A. Gruzberg, and F. Evers, *Phys. Rev. Lett.* **109**, 206804 (2012).
- [27] A. Del Maestro, B. Rosenow, J. A. Hoyos, and T. Vojta, *Phys. Rev. Lett.* **105**, 145702 (2010).
- [28] C. Wang, B. Lian, X. M. Guo, J. H. Mao, Z. T. Zhang, D. Zhang, B. L. Gu, Y. Xu, and W. H. Duan, *Phys. Rev. Lett.* **123**, 126402 (2019).
- [29] Y. Liu, Z. Wang, X. Zhang, C. Liu, Y. Liu, Z. Zhou, J. Wang, Q. Wang, Y. Liu, C. Xi, M. Tian, H. Liu, J. Feng, X. C. Xie, and J. Wang, *Phys. Rev. X* **8**, 021002 (2018).
- [30] C. Liu, C. S. Lian, M. H. Liao, Y. Wang, Y. Zhong, C. Ding, W. Li, C. L. Song, K. He, X. C. Ma, W. H. Duan, D. Zhang, Y. Xu, L. L. Wang, and Q. K. Xue, *Phys. Rev. Mater.* **2**, 094001 (2018).
- [31] C. Huang, E. Zhang, Y. Zhang, J. Zhang, F. Xiu, H. Liu, X. Xie, L. Ai, Y. Yang, M. Zhao, J. Qi, L. Li, S. Liu, Z. Li, R. Zhan, Y.-Q. Bie, X. Kou, S. Deng, and X. C. Xie, [arXiv:2010.12775](https://arxiv.org/abs/2010.12775).